K.A. Hamed and N. Sadati (*Intelligent Systems Laboratory, Electrical Engineering Department, Sharif University of Technology, Tehran, Iran*)

E-mail: sadati@sharif.edu

W.A. Gruver (*School of Engineering Science, Simon Fraser University, Burnaby, BC V5A 1S6, Canada*)

N. Sadati and G.A. Dumont (*Department of Electrical and Computer Engineering, The University of British Columbia, Vancouver BC V6T 1Z4, Canada*)

References

1 Grizzle, J.W., Abba, G., and Plestan, F.: 'Asymptotically stable walking for biped robots: analysis via systems with impulse effects', *IEEE Trans. Autom. Control*, 2001, **46**, (1), pp. 51–64
2 Westervelt, E.R., Grizzle, J.W., Chevallereau, C., Choi, J.H., and Morris, B.: 'Feedback control of dynamic bipedal robot locomotion' (CRC Press, Boca Raton, USA, June 2007)
3 Grizzle, J.W., Westervelt, E.R., and Canudas, C.: 'Event-based PI control of an underactuated biped walker'. Proc. of 2003 IEEE Int. Conf. on Decision and Control, Maui, HI, USA, 2003, pp. 3091–3096
4 Westervelt, E.R., Grizzle, J.W., and Canudas, C.: 'Switching and PI control of walking motions of planar biped walkers', *IEEE Trans. Autom. Control*, 2003, **48**, (2), pp. 308–312
5 Grizzle, J.W.: 'Remarks on event-based stabilization of periodic orbits in systems with impulse effects'. 2nd Int. Symp. on Communications, Control and Signal Processing, Marrakech, Morocca, 2006
6 Parker, T.S., and Chua, L.O.: 'Practical numerical algorithms for chaotic systems' (Springer-Verlag, New York, USA, 1989)

Significant step in ultra-high stability quartz crystal oscillators

P. Salzenstein, A. Kuna, L. Sojdr and J. Chauvin

The best frequency stability ever measured on a quartz crystal oscillator is reported: this new Boitiers à Vieillissement Amélioré (BVA) oscillator has an estimated flicker frequency modulation floor of 2.5×10^{-14} at 5 MHz.

Introduction: It is generally supposed that the resonator is the main limiting element on the ability to manufacture ultra-high stability quartz oscillators. Fabrication processes of SC-cut quartz resonators have now enough maturity, and allow achieving ultra-low noise crystal resonators. To choose the best resonator, a tool can be used to sort out the best resonators showing its capability to be integrated into the best oscillator design [1]. Hence the new step presented in the first part consists in working on the resonator environment. As far as $1/f$ noise of the amplifiers and temperature variation around the turnover point seems to be the two main limiting factors on the electronics contribution to the frequency stability of the oscillator, it is necessary to optimise the design of the oscillator to decrease the noise. The latter part of this Letter presents performance on oscillators in terms of ultra-high frequency stability and state-of-the-art obtained results.

Main limitation on frequency stability of oscillator: The frequency stability is determined by the crystal's loaded quality factor (Q_L). It is inversely dependent on the frequency, and is dependent on the particular cut. The temperature sensitivity depends primarily on the cut. The temperature compensated cuts are chosen as to minimise frequency and temperature dependencies [2]. The stress compensated (SC) cut is less sensitive to mechanical stresses. It is a double-rotated cut for oven-stabilised oscillators with low phase noise and good aging characteristics and low sensitivity to drive level dependency [3]. Hence, the chosen resonator (serial number: 4304048SN35) manufactured by the Oscilloquartz Company in 2010 is placed in an appropriate thermostat [4] in the first prototype of an oven-controlled crystal oscillator (OCXO) called 8607-C. It consists of a new Boitiers à Vieillissement Amélioré (BVA) type oscillator where electrodes are deposited not on the resonator itself but on inner sides of two condenser discs made of adjacent slices of the quartz from the same bar, forming a three-layer sandwich with no stress between the electrodes and the vibrating element. Turnover temperature of the resonator is 88.6°C. The unloaded Q factor is 2.63×10^6. Regarding experimental phase noise measurements, Q_L can be given by the 1.6 Hz intercept point between the $1/f$ slope (phase flicker noise) and the $1/f^3$ slope (frequency flicker noise). $Q_L = 1.57 \times 10^6$. Thermostats are especially developed by Oscilloquartz with a double oven for this new model, with drastic optimisation. Electronics circuits are entirely renewed to reduce the contribution of the $1/f$ noise of the amplification elements [5], considering the goal is to decrease the $1/\tau$ curve in the time domain, where τ is the integration time.

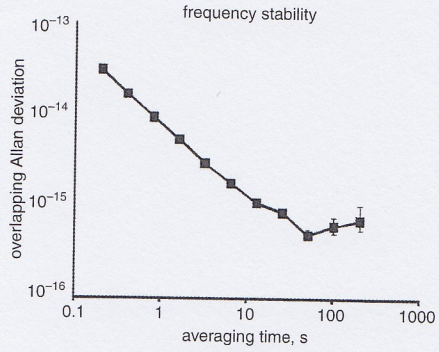

Fig. 1 *IPE 3 bench limit*

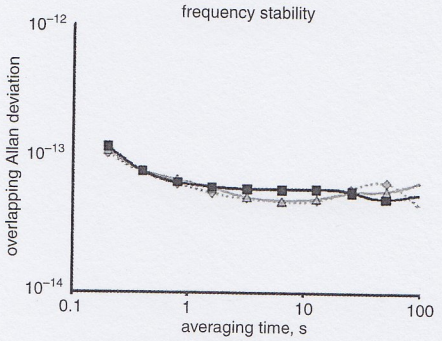

Fig. 2 *Frequency stability for each pair of oscillators: 543-567 (■), 567-8607C (◆), 543-8607C (▲)*

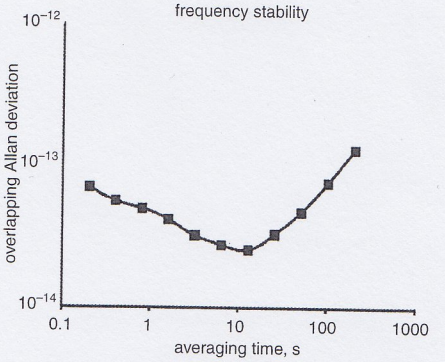

Fig. 3 *Overlapping Allan deviation of 8607-C oscillator deduced by three-cornered hat analysis*

Frequency stability measurements on new oscillator: Determination of the short-term frequency stability of the new oscillator is performed thanks to a dual mixer time difference multiplication (DMTDM) [6] based 'IPE3' system developed at the Institute of Photonics and Electronics (IPE) in Prague, with a beat frequency of 5 Hz, where each measure gives 5000 samples separated by a basic 200 ms integration time [7]. The frequency stability limit of the IPE3 bench is determined with the rejection of one BVA oscillator. Then it is possible to deduce a flicker phase of respectively 8×10^{-15} and 1.1×10^{-15} at 1 and 13 s. The limit of the IPE3 bench is presented in Fig. 1. The contribution of the instrumentation can be negligible between 0.2 and 100 s where the flicker frequency modulation (FFM) floor is expected. To determine the frequency stability of the 8607-C prototype, it is measured with two other ultra-stable BVA oscillators, respectively serial numbers 543 and 567. Fig. 2 presents the frequency stability curves obtained for each pair of oscillators. The contribution of each oscillator is deduced for every measure performed on each pair by the three-cornered hat analysis [8]. One can note that, even if the two oscillators referenced 543 and 567 are much more

stable in terms of aging, the new one has the best FFM floor. The curve represented in Fig. 3 shows that the frequency stability of the 8607-C prototype is less than 4.5×10^{-14} for integration times between 1 and 50 s. The FFM floor is determined to be equal to 2.5×10^{-14} for an integration time around 10 s. Estimated uncertainty is equal to $\pm 3 \times 10^{-15}$ [9].

Conclusion: This new prototype of a 5 MHz 8607-C BVA oscillator, with a highly optimised double oven and low noise electronics, presents the best FFM floor ever measured on a BVA quartz oscillator, at 2.5×10^{-14}. Since the limit of 8×10^{-14} for the available FFM floor on commercial quartz oscillators is for the first time in the last 15 years significantly reduced, this new step in quartz oscillators opens new hope to approach 10^{-14} ultra-high stability oscillators.

5 July 2010
doi: 10.1049/el.2010.1828

P. Salzenstein (*Franche Comté Eléctronique Thermique Optique Sciences et Technologies, CNRS, 26 Chemin de l'épitaphe, Besançon F25000, France*)

E-mail: patrice.salzenstein@femto-st.fr

A. Kuna and L. Sojdr (*Institute of Photonics and Electronics, Academy of Sciences, Chaberska 57, 18251 Prague 8, Czech Republic*)

J. Chauvin (*Oscilloquartz, 16 rue des Brevards, Neuchâtel 2002, Switzerland*)

References

1 Salzenstein, P., Kuna, A., Sojdr, L., Sthal, F., Cholley, N., and Lefebvre, F.: 'Frequency stability measurements of ultra-stable BVA resonators and oscillators', *Electron. Lett.*, 2010, **46**, (10), pp. 686–688
2 Norton, J.R., Cloeren, J.M., and Sulzer, P.G.: 'Brief history of the development of ultra-precise oscillators for ground and space applications'. Proc. IEEE Int. Frequency Control Symp., Honolulu, HI, USA, 1996, pp. 47–57
3 Brendel, R., Addouche, M., Salzenstein, P., Rubiola, E., and Shmaliy, Y.S.: 'Drive level dependence in quartz crystal resonators at low drive levels: a review'. Proc. 18th European Frequency and Time Forum, Guilford, UK, IEE Conf. Pub., Guildford, UK, CP499, 2004, pp. 11–18
4 Sthal, F., Galliou, S., Abbe, P., Vacheret, X., and Cibiel, G.: 'Ultra-stable crystal ovens and simple characterisation', *Electron. Lett.*, 2007, **43**, (16), pp. 900–901
5 Walls, F.L.: 'The quest to understand and reduce 1/f noise in amplifiers and BAW quartz oscillators'. Proc. 9th European Frequency and Time Forum, Besançon, France, 1995, pp. 227–240
6 Brida, G.: 'High resolution frequency stability measurement system', *Rev. Sci. Instrum.*, 2002, **73**, (5), pp. 2171–2174
7 Kuna, A., Cermak, J., Sojdr, L., Salzenstein, P., and Lefebvre, F.: 'Lowest flicker-frequency floor measured on BVA oscillators', *IEEE Trans. Ultrason. Ferroelectr. Freq. Control.*, 2010, **57**, (3), pp. 548–551
8 Allan, D.W.: 'Time and frequency (time domain) characterization, estimation, and prediction of precision clocks and oscillators', *IEEE Trans. Ultrason. Ferroelectr. Freq. Control.*, 1987, **34**, (6), pp. 647–654
9 Ekstrom, C.R., and Koppang, P.A.: 'Error bars for three-cornered hats', *IEEE Trans. Ultrason. Ferroelectr. Freq. Control.*, 2006, **53**, (5), pp. 876–879

Stripe-based connected components labelling

H.L. Zhao, Y.B. Fan, T.X. Zhang and H.S. Sang

A fast stripe-based connected component labelling algorithm is proposed for binary image labelling. Stripe extraction strategy is used to transform the pixel-connected issues, which most of the previously proposed algorithms focused on, into stripe-connected issues. The stripe-union strategy treats the combination of the neighbouring stripes as the mergence of rooted trees. Finally, comparisons are performed with other famous fast labelling algorithms. The proposed algorithm has shown better performance than the state-of-the-art algorithm in real images test, while the auxiliary memory is not required at all compared with all competitors.

Introduction: Labelling connected components in a binary image is one of the most fundamental tasks in image processing and pattern recognition. Unfortunately, owing to the complex connectivity possibilities of the connected components in images, labelling is a time-consuming process and cannot be simply divided into parallel local operations without any global consideration. In recent years, several famous labelling strategies have been proposed for speed-up of the labelling process [1–4]. Although these techniques obtain great performance, there is still room for acceleration. Furthermore, the common disadvantage of proposed algorithms is that the auxiliary memory space is needed for their intermediate data which is often very large especially for high resolution images.

In this Letter, a fast and memory-free stripe-based connected component labelling algorithm (SBLA) is presented. High-performance for the labelling process is obtained while extra auxiliary memory is not required. Unlike other labelling algorithms based on pixel neighbourhood examination, the SBLA takes the contiguous pixels in two rows as stripes. The equivalent connected components merge process is performed between stripes. So the efficiency of neighbourhood examination is greatly improved and the merge time is significantly reduced.

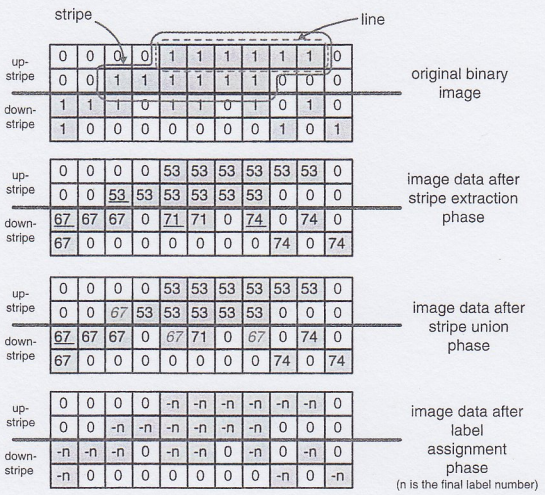

Fig. 1 *Illustration for SBLA*
Part of 16 × 16 image example illustration for SBLA

Preliminary: To simplify the problem and better illustrate the algorithm, we presume the binary image (where the original image is binarised into the foreground and background) is N × M, where N is the number of columns; M is the number of rows and is even. If M is odd, then a row of background value is appended to the original image, which will have an even number of rows, and the problem will be made equivalent to the previous assumption. The foreground value of the binary image is 1, and the background is 0. The SBLA is composed of three phases: stripes extraction and representation, stripes union, label assignment.

Stripe extraction and representation: In this phase, we take every even row with the following odd row as a work-region. The aim of this phase is to extract and represent the connected components in every work-region. In our scheme, we call these connected components stripes. The steps to obtain the stripes are as follows:

Step 1: Fetch out two pixels $P_i(x_i, y_i)$ and $P_j(x_i, y_i + 1)$ from the current work-region every time.
Step 2: If the two pixels' values are both 0, return to step 1. If one of two is non-zero, the global position value of this non-zero pixel $G(P_i)$ is assigned to itself, i.e. $P_i(x_i, y_i) = G(P_i) = y_i \times N + x_i$. If both pixels are non-zero, they are assigned the global position value of the one in the odd row.
Step 3: Continue to fetch out the next two pixels. If at least one pixel is non-zero, assign the previous $G(P_i)$ to the non-zero pixel, and then repeat step 3. If both pixels are 0, return to step 1 directly.

These steps are continued until the whole image has been traversed. The second part of Fig. 1*b* is one example illustration for the result of the first phase of the SBLA. From the steps mentioned above, we can get the properties of stripe. Suppose a stripe S is extracted from r and $r + 1$ rows, where r is even, then the stripe S has the following properties: